Quantum Phase Transitions

Subir Sachdev
Department of Physics
Harvard University
Cambridge, MA 02138
USA
E-mail: subir_sachdev@harvard.edu

March 21, 2006

To appear in
Handbook of Magnetism and Advanced Magnetic Materials,
edited by H. Kronmuller and S. Parkin.

1 Introduction

The study of quantum phase transitions has been a major focus of theoretical and experimental work in systems of correlated electrons and in correlated ultracold atoms in recent years. However, some of the best characterized and understood examples of quantum phase transitions are found in magnetic materials. These therefore serve as a valuable laboratory for testing our understanding of real systems in the vicinity of quantum critical points. We will review some of the simplest model systems below, along with their experimental realizations. This will be followed by a discussion of recent theoretical advances on some novel quantum critical points displayed by quantum magnets which have no direct analog in the theory of classical phase transitions at finite temperature (T). Portions of this article have been adapted from another recent review by the author [a].

In all the magnetic systems considered below, there is at least one ground state in which the symmetry of spin rotations is broken. So in this phase we have

$$\langle \hat{S}_j^\alpha \rangle \neq 0. \tag{1}$$

at $T = 0$. Here $\hat{S}$ is the electron spin operator on site j, and $\alpha = x, y, z$ are the spin components. In all cases we consider here the Hamiltonian has at least a symmetry of spin inversion, and this symmetry is broken by (1). We are quite familiar with such magnetic systems, as all antiferromagnets, ferromagnets, or even spin glasses obey (1) at sufficiently low temperatures.

Let us now try to access a *paramagnetic* phase where

$$\langle \hat{S}_j^\alpha \rangle = 0. \tag{2}$$

Normally, we do this by raising temperature. The resulting phase transition between phases characterized by (1) and (2) is well understood, and described by the well-developed theory of classical phase transitions. This shall *not* be our interest here. Rather, we are interested in moving from magnetic system obeying (1), to a *quantum paramagnet* obeying (2), by varying a system parameter at $T = 0$. There are many experimental and theoretical examples of such transitions: at the critical point, there is a qualitative change in the nature of the quantum wavefunction of the ground state.

One crucial feature of quantum phase transitions is that (2) is usually *not* sufficient to characterize the paramagnetic phase. In the Landau-Ginzburg-Wilson (LGW) approach to classical phase transitions, one focuses on the broken symmetry associated with (1), and defines a corresponding order parameter. A field theory of thermal fluctuations of this order parameter is then sufficient to describe the transition to the paramagnetic phase, and also to completely characterize the paramagnet. As we will discuss in Section 4, this procedure is not sufficient in some of the most interesting and physically important quantum phase transitions. The paramagnetic phase is not completely characterized by (2), and typically breaks some other symmetry of the Hamiltonian, or has a more subtle 'topological' order. Furthermore, this additional 'order' of the paramagnet plays an important role in the theory of the quantum critical point.

We will begin in Section 2 by introducing some simple lattice models, and their experimental realizations, which exhibit quantum phase transitions. The theory of the critical point in these models is based upon a natural

extension of the LGW method, and this will be presented in Section 3. This section will also describe the consequences of a zero temperature critical point on the non-zero temperature properties. Section 4 will consider more complex models in which quantum interference effects play a more subtle role, and which cannot be described in the LGW framework: such quantum critical points are likely to play a central role in understanding many of the correlated electron systems of current interest.

2 Simple models

2.1 Ising ferromagnet in a transverse field

This quantum phase transition is realized [b] in the insulator $LiHoF_4$. The Ho ion has a $S = 1/2$ Ising spin which prefers to orient itself either parallel or anti-parallel to a particular crystalline axis (say z). These Ising spins interact via the magnetic dipolar coupling and normally form a ferromagnetic ground state which obeys (1) for $\alpha = z$. As we describe below, upon application of a (transverse) magnetic field in the plane perpendicular to the z axis, quantum fluctuations of the Ising spin are enhanced, and there is eventually a quantum phase transition to a paramagnetic state obeying (2) for $\alpha = z$.

Rather than explore the full complexity of the experimentally relevant model, we will restrict our attention to a simple one-dimensional model, with nearest neighbor couplings, which displays much of the same physics. The dynamics of this quantum Ising spin chain is described by the simple Hamiltonian

$$H_I = -J \sum_{j=1}^{N-1} \hat{\sigma}_j^z \hat{\sigma}_{j+1}^z - gJ \sum_{j=1}^{N} \hat{\sigma}_j^x, \tag{3}$$

where $\hat{\sigma}_j^\alpha$ are the Pauli matrices which act on the Ising spin degrees of freedom ($\hat{S}_j^\alpha \propto \hat{\sigma}_j^\alpha$) $J > 0$ is the ferromagnetic coupling between nearest neighbor spins, and $g \geq 0$ is a dimensionless coupling constant which determines the strength of the transverse field. In the thermodynamic limit ($N \to \infty$), the ground state of H_I exhibits a second-order quantum phase transition as g is tuned across a critical value $g = g_c$ (for the specific case of H_I it is known that $g_c = 1$), as we will now illustrate.

First, consider the ground state of H_I for $g \ll 1$. At $g = 0$, there are two degenerate *ferromagnetically ordered* ground states

$$|\Uparrow\rangle = \prod_{j=1}^{N} |\uparrow\rangle_j \quad ; \quad |\Downarrow\rangle = \prod_{j=1}^{N} |\downarrow\rangle_j \tag{4}$$

Each of these states breaks a discrete 'Ising' symmetry of the Hamiltonian– rotations of all spins by 180 degrees about the x axis. These states are more succinctly characterized by defining the ferromagnetic moment, N_0 by

$$N_0 = \langle\Uparrow| \hat{\sigma}_j^z |\Uparrow\rangle = -\langle\Downarrow| \hat{\sigma}_j^z |\Downarrow\rangle \tag{5}$$

At $g = 0$ we clearly have $N_0 = 1$. A key point is that in the thermodynamic limit, this simple picture of the ground state survives for a finite range of small g (indeed, for all $g < g_c$), but with $0 < N_0 < 1$. The quantum tunnelling between the two ferromagnetic ground states is exponentially small in N (and so can be neglected in the thermodynamic limit), and so the ground state remains two-fold degenerate and the discrete Ising symmetry remains broken. The change in the wavefunctions of these states from Eq. (4) can be easily determined by perturbation theory in g: these small g quantum fluctuations reduce the value of N_0 from unity but do not cause the ferromagnetism to disappear.

Now consider the ground state of H_I for $g \gg 1$. At $g = \infty$ there is a single *non*-degenerate ground state which fully preserves all symmetries of H_I:

$$|\Rightarrow\rangle = 2^{-N/2} \prod_{j=1}^{N} \left(|\uparrow\rangle_j + |\downarrow\rangle_j \right). \tag{6}$$

It is easy to verify that this state has no ferromagnetic moment $N_0 = \langle\Rightarrow| \hat{\sigma}_j^z |\Rightarrow\rangle = 0$. Further, perturbation theory in $1/g$ shows that these features of the ground state are preserved for a finite range of large g values (indeed, for all $g > g_c$). One can visualize this ground state as one in which strong quantum fluctuations have destroyed the ferromagnetism, with the local magnetic moments quantum tunnelling between 'up' and 'down' on a time scale of order $\hbar/J$.

Given the very distinct signatures of the small g and large g ground states, it is clear that the ground state cannot evolve smoothly as a function of g.

These must be at least one point of non-analyticity as a function of g: for H_I it is known that there is only a single non-analytic point, and this is at the location of a second-order quantum phase transition at $g = g_c = 1$.

The character of the excitations above the ground state also undergoes a qualitative change across the quantum critical point. In both the $g < g_c$ and $g > g_c$ phase these excitations can be described in the Landau *quasiparticle* scheme *i.e.* as superpositions of nearly independent particle-like excitations; a single well-isolated quasiparticle has an infinite lifetime at low excitation energies. However, the physical nature of the quasiparticles is very different in the two phases. In the ferromagnetic phase, with $g < g_c$, the quasiparticles are domain walls between regions of opposite magnetization:

$$|j, j+1\rangle = \prod_{k=1}^{j} |\uparrow\rangle_k \prod_{\ell=j+1}^{N} |\downarrow\rangle_\ell \tag{7}$$

This is the exact wavefunction of a stationary quasiparticle excitation between sites j and $j+1$ at $g = 0$; for small non-zero g the quasiparticle acquires a 'cloud' of further spin-flips and also becomes mobile. However the its qualitative interpretation as a domain wall between the two degenerate ground states remains valid for all $g < g_c$. In contrast, for $g > g_c$, there is no ferromagnetism, and the non-degenerate paramagnetic state has a distinct quasiparticle excitation:

$$|j\rangle = 2^{-N/2} \left(|\uparrow\rangle_j - |\downarrow\rangle_j \right) \prod_{k \neq j} \left(|\uparrow\rangle_k + |\downarrow\rangle_k \right). \tag{8}$$

This is a stationary 'flipped spin' quasiparticle at site j, with its wavefunction exact at $g = \infty$. Again, this quasiparticle is mobile and applicable for all $g > g_c$, but there is no smooth connection between Eq. (8) and (7).

2.2 Coupled dimer antiferromagnet

Now we consider a model of $S = 1/2$ spins which interact via an antiferromagnetic exchange, and the Hamiltonian has full SU(2) spin rotation invariance. Physically, the cuprates are by far the most important realization of Hamiltonians in this class. However, rather than facing the daunting complexity of those compounds, it is useful to study simpler insulators in which

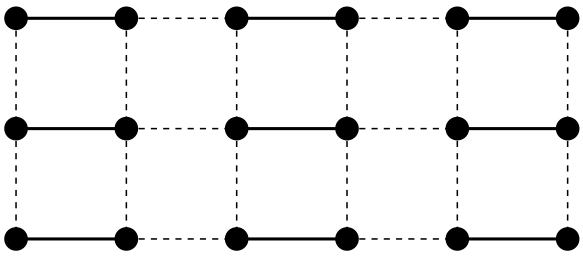

Figure 1: The coupled dimer antiferromagnet. Qubits (*i.e.* $S = 1/2$ spins) are placed on the sites, the $\mathcal{A}$ links are shown as full lines, and the $\mathcal{B}$ links as dashed lines.

a quantum phase transition from an antiferromagnet to a paramagnet can be explored. One experimentally and theoretically well studied system [c, d, e, f] is $TlCuCl_3$. Here the $S = 1/2$ spins reside on the Cu^+ ions, which reside in a rather complicated spatial arrangement. As in Section 2.1, we will not explore the full complexity of the experimental magnet, but be satisfied with a caricature that captures the essential physics. The most important feature of the crystal structure of $TlCuCl_3$ (as will become clear in Section 4) is that it is naturally *dimerized i.e.* there is a pairing between Cu spins which respects all symmetries of the crystal structure. So will consider the simplest dimer antiferromagnet of $S = 1/2$ spins which exhibits a quantum phase transition essentially equivalent to that found in $TlCuCl_3$.

The Hamiltonian of the dimer antiferromagnet is illustrated in Fig 1 and is given by

$$\begin{aligned} H_d &= J \sum_{\langle jk \rangle \in A} \left(\hat{\sigma}_j^x \hat{\sigma}_k^x + \hat{\sigma}_j^y \hat{\sigma}_k^y + \hat{\sigma}_j^z \hat{\sigma}_k^z \right) \\ &+ \frac{J}{g} \sum_{\langle jk \rangle \in B} \left(\hat{\sigma}_j^x \hat{\sigma}_k^x + \hat{\sigma}_j^y \hat{\sigma}_k^y + \hat{\sigma}_j^z \hat{\sigma}_k^z \right), \end{aligned} \tag{9}$$

where now $J > 0$ is the antiferromagnetic exchange constant, $g \geq 1$ is the dimensionless coupling, and the set of nearest-neighbor links $\mathcal{A}$ and $\mathcal{B}$ are defined in Fig 1. An important property of H_d is that it is now invariant under the full SU(2) group of spin rotations under which the $\hat{\sigma}^\alpha$ transform as ordinary vectors (in contrast to the Z_2 symmetry group of H_I). In analogy with H_I, we will find that H_d undergoes a quantum phase transition from a paramagnetic phase which preserves all symmetries of the Hamiltonian at

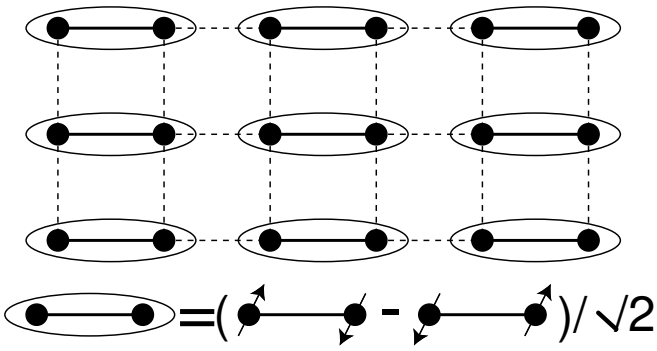

Figure 2: The paramagnetic state of H_d for $g > g_c$. The state illustrated is the exact ground state for $g = \infty$, and it is adiabatically connected to the ground state for all $g > g_c$.

large g, to an *antiferromagnetic* phase which breaks the SU(2) symmetry at small g. This transition occurs at a critical value $g = g_c$, and the best current numerical estimate is [g] $1/g_c = 0.52337(3)$.

As in the previous subsection, we can establish the existence of such a quantum phase transition by contrasting the disparate physical properties at large g with those at $g \approx 1$. At $g = \infty$ the exact ground state of H_d is

$$|\text{spin gap}\rangle = \prod_{\langle jk\rangle \in A} \frac{1}{\sqrt{2}} \left(|\uparrow\rangle_j |\downarrow\rangle_k - |\downarrow\rangle_j |\uparrow\rangle_k \right) \tag{10}$$

and is illustrated in Fig 2. This state is non-degenerate and invariant under spin rotations, and so is a paramagnet: the qubits are paired into spin singlet valence bonds across all the $\mathcal{A}$ links. The excitations above the ground state are created by breaking a valence bond, so that the pair of spins form a spin triplet with total spin $S = 1$ — this is illustrated in Fig 3. It costs a large energy to create this excitation, and at finite g the triplet can hop from link to link, creating a gapped *triplon* quasiparticle excitation. This is similar to the large g paramagnet for H_I, with the important difference that each quasiparticle is now 3-fold degenerate.

At $g = 1$, the ground state of H_d is not known exactly. However, at this point H_d becomes equivalent to the nearest-neighbor square lattice antiferromagnet, and this is known to have antiferromagnetic order in the ground state, as illustrated in Fig 4. This state is similar to the ferromagnetic ground

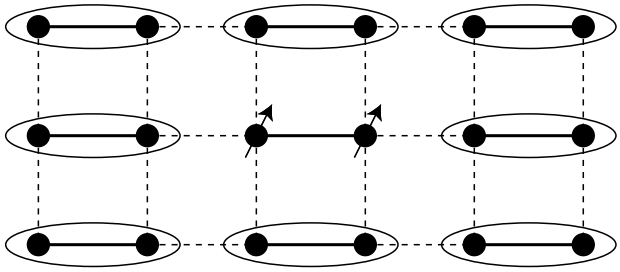

Figure 3: The triplon excitation of the $g > g_c$ paramagnet. The stationary triplon is an eigenstate only for $g = \infty$ but it becomes mobile for finite g.

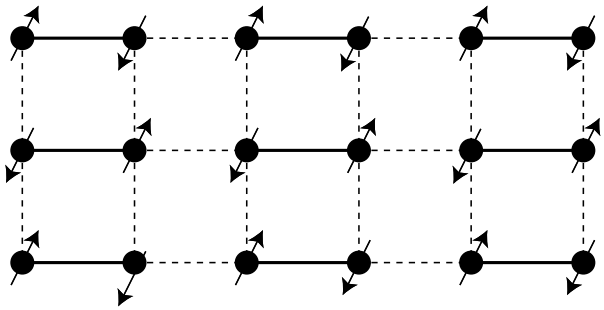

Figure 4: Schematic of the ground state with antiferromagnetic order with $g < g_c$.

state of H_I, with the difference that the magnetic moment now acquires a staggered pattern on the two sublattices, rather than the uniform moment of the ferromagnet. Thus in this ground state

$$\langle \mathrm{AF} | \, \hat{\sigma}_j^\alpha \, | \mathrm{AF} \rangle = N_0 \eta_j n_\alpha \tag{11}$$

where $0 < N_0 < 1$ is the antiferromagnetic (or Néel) moment, $\eta_j = \pm 1$ identifies the two sublattices in Fig 4, and n_α is an arbitrary unit vector specifying the orientation of the spontaneous magnetic moment which breaks the O(3) spin rotation invariance of H_d. The excitations above this antiferromagnet are also distinct from those of the paramagnet: they are a *doublet* of spin waves consisting of a spatial variation in the local orientation, n_α, of the antiferromagnetic order: the energy of this excitation vanishes in the limit of long wavelengths, in contrast to the finite energy gap of the triplon excitation of the paramagnet.

As with H_I, we can conclude from the distinct characters of the ground states and excitations for $g \gg 1$ and $g \approx 1$ that there must be a quantum critical point at some intermediate $g = g_c$.

3 Quantum criticality

The simple considerations of Section 2 have given a rather complete description (based on the quasiparticle picture) of the physics for $g \ll g_c$ and $g \gg g_c$. We turn, finally, to the region $g \approx g_c$. For the specific models discussed in Section 2, a useful description is obtained by a method that is a generalization of the LGW method developed earlier for thermal phase transitions. However, some aspects of the critical behavior (*e.g.* the general forms of Eqns (14), (15), and (16)) will apply also to the quantum critical point of Section 4.

Following the canonical LGW strategy, we need to identify a collective order parameter which distinguishes the two phases. This is clearly given by the ferromagnetic moment in Eq. (5) for the quantum Ising chain, and the antiferromagnetic moment in Eq. (11) for the coupled dimer antiferromagnet. We coarse-grain these moments over some finite averaging region, and at long wavelengths this yields a real order parameter field ϕ_α, with the index $\alpha = 1 \ldots n$. For the Ising case we have $n = 1$ and ϕ_α is a measure of the local

average of N_0 as defined in Eq. (5). For the antiferromagnet, a extends over the three values x, y, z (so $n = 3$), and three components of ϕ_α specify the magnitude and orientation of the local antiferromagnetic order in Eq. (11); note the average orientation of a specific spin at site j is η_j times the local value of ϕ_α.

The second step in the LGW approach is to write down a general field theory for the order parameter, consistent with all symmetries of the underlying model. As we are dealing with a quantum transition, the field theory has to extend over *spacetime*, with the temporal fluctuations representing the sum over histories in the Feynman path integral approach. With this reasoning, the proposed partition function for the vicinity of the critical point takes the following form

$$\mathcal{Z}_\phi = \int \mathcal{D}\phi_\alpha(x,\tau) \exp\Big[- \int d^d x d\tau \left(\frac{1}{2} \left((\partial_\tau \phi_\alpha)^2 + c^2 (\nabla_x \phi_\alpha)^2 + s \phi_\alpha^2 \right) + \frac{u}{4!} \left(\phi_\alpha^2 \right)^2 \right) \Big]. \tag{12}$$

Here τ is imaginary time, there is an implied summation over the n values of the index a, c is a velocity, and s and $u > 0$ are coupling constants. This is a field theory in $d + 1$ spacetime dimensions, in which the Ising chain corresponds to $d = 1$ and the dimer antiferromagnet to $d = 2$. The quantum phase transition is accessed by tuning the "mass" s: there is a quantum critical point at $s = s_c$ and the $s < s_c$ ($s > s_c$) regions corresponds to the $g < g_c$ ($g > g_c$) regions of the lattice models. The $s < s_c$ phase has $\langle \phi_\alpha \rangle \neq 0$ and this corresponds to the spontaneous breaking of spin rotation symmetry noted in Eqs. (5) and (11) for the lattice models. The $s > s_c$ phase is the paramagnet with $\langle \phi_\alpha \rangle = 0$. The excitations in this phase can be understood as small harmonic oscillations of ϕ_α about the point (in field space) $\phi_\alpha = 0$. A glance at Eqn (12) shows that there are n such oscillators for each wavevector. These oscillators clearly constitute the $g > g_c$ quasiparticles found earlier in Eqn (8) for the Ising chain (with $n = 1$) and the triplon quasiparticle (with $n = 3$) illustrated in Fig 3) for the dimer antiferromagnet.

We have now seen that there is a perfect correspondence between the phases of the quantum field theory $\mathcal{Z}_\phi$ and those of the lattice models H_I and H_d. The power of the representation in Eqn. (12) is that it also allows us to get a simple description of the quantum critical point. In particular, readers may already have noticed that if we interpret the temporal direction τ in Eqn. (12)

as another spatial direction, then $\mathcal{Z}_\phi$ is simply the classical partition function for a thermal phase transition in a ferromagnet in $d+1$ dimensions: this is the canonical model for which the LGW theory was originally developed. We can now take over standard results for this classical critical point, and obtain some useful predictions for the quantum critical point of $\mathcal{Z}_\phi$. It is useful to express these in terms of the dynamic susceptibility defined by

$$\chi(k,\omega) = \frac{i}{\hbar}\int d^d x \int_0^\infty dt \left\langle \left[\hat{\phi}(x,t), \hat{\phi}(0,0)\right]\right\rangle_T e^{-ikx+i\omega t}. \tag{13}$$

Here $\hat{\phi}$ is the Heisenberg field operator corresponding to the path integral in Eqn. (12), the square brackets represent a commutator, and the angular brackets an average over the partition function at a temperature T. The structure of χ can be deduced from the knowledge that the quantum correlators of $\mathcal{Z}_\phi$ are related by analytic continuation in time to the corresponding correlators of the classical statistical mechanics problem in $d+1$ dimensions. The latter are known to diverge at the critical point as $\sim 1/p^{2-\eta}$ where p is the $(d+1)-$dimensional momentum, η is defined to be the anomalous dimension of the order parameter ($\eta = 1/4$ for the quantum Ising chain). Knowing this, we can deduce the form of the quantum correlator in Eq. (13) at the zero temperature quantum critical point

$$\chi(k,\omega) \sim \frac{1}{(c^2k^2-\omega^2)^{1-\eta/2}} \quad ; \quad T=0,\ g=g_c. \tag{14}$$

The most important property of Eq. (14) is the absence of a quasiparticle pole in the spectral density. Instead, $\mathrm{Im}\,(\chi(k,\omega))$ is non-zero for all $\omega > ck$, reflecting the presence of a continuum of critical excitations. Thus the stable quasiparticles found at low enough energies for all $g \neq g_c$ are absent at the quantum critical point.

We now briefly discuss the nature of the phase diagram for $T > 0$ with g near g_c. In general, the interplay between quantum and thermal fluctuations near a quantum critical point can be quite complicated [h], and we cannot discuss it in any detail here. However, the physics of the quantum Ising chain is relatively simple, and also captures many key features found in more complex situations, and is summarized in Fig 5. For all $g \neq g_c$ there is a range of low temperatures ($T \lesssim |g-g_c|$) where the long time dynamics can be described using a dilute gas of thermally excited quasiparticles. Further, the dynamics of these quasiparticles is quasiclassical, although we reiterate

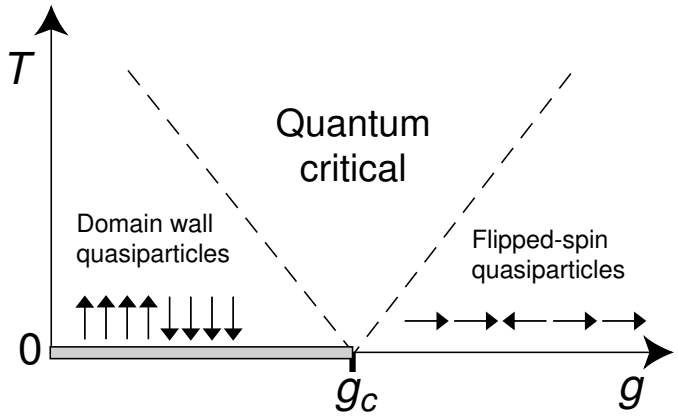

Figure 5: Nonzero temperature phase diagram of H_I. The ferromagnetic order is present only at $T = 0$ on the shaded line with $g < g_c$. The dashed lines at finite T are crossovers out of the low T quasiparticle regimes where a quasiclassical description applies. The state sketched on the paramagnetic side used the notation $|{\rightarrow}\rangle_j = 2^{-1/2}(|{\uparrow}\rangle_j + |{\downarrow}\rangle_j)$ and $|{\leftarrow}\rangle_j = 2^{-1/2}(|{\uparrow}\rangle_j - |{\downarrow}\rangle_j)$.

that the nature of the quasiparticles is entirely distinct on opposite sides of the quantum critical point. Most interesting, however, is the novel *quantum critical* region, $T \gtrsim |g - g_c|$, where neither quasiparticle picture nor a quasiclassical description are appropriate. Instead, we have to understand the influence of temperature on the critical continuum associated with Eq. (14). This is aided by scaling arguments which show that the only important frequency scale which characterizes the spectrum is $k_B T/\hbar$, and the crossovers near this scale are universal *i.e.* independent of specific microscopic details of the lattice Hamiltonian. Consequently, the zero momentum dynamic susceptibility in the quantum critical region takes the following form at small frequencies:

$$\chi(k = 0, \omega) \sim \frac{1}{T^{2-\eta}} \frac{1}{(1 - i\omega/\Gamma_R)}. \tag{15}$$

This has the structure of the response of an overdamped oscillator, and the damping frequency, Γ_R, is given by the universal expression

$$\Gamma_R = \left(2 \tan \frac{\pi}{16}\right) \frac{k_B T}{\hbar} \tag{16}$$

The numerical proportionality constant in Eqn. (16) is specific to the quantum Ising chain; other models also obey Eqn. (16) but with a different nu-

merical value for this constant.

4 Beyond LGW theory

The quantum transitions discussed so far have turned to have a critical theory identical to that found for classical thermal transitions in $d+1$ dimensions. Over the last decade it has become clear that there are numerous models, of key physical importance, for which such a simple classical correspondence does not exist. In these models, quantum *Berry phases* are crucial in establishing the nature of the phases, and of the critical boundaries between them. In less technical terms, a signature of this subtlety is an important simplifying feature which was crucial in the analyses of Section 2: both models had a straightforward $g \to \infty$ limit in which we were able to write down a simple, non-degenerate, ground state wavefunction of the 'disordered' paramagnet. In many other models, identification of the 'disordered' phase is not as straightforward: specifying absence of a particular magnetic order as in (2) is *not* enough to identify a quantum state, as we still need to write down a suitable wavefunction. Often, subtle quantum interference effects induce new types of order in the 'disordered' state, and such effects are entirely absent in the LGW theory.

An important example of a system displaying such phenomena is the $S = 1/2$ square lattice antiferromagnet with additional frustrating interactions. The quantum degrees of freedom are identical to those of the coupled dimer antiferromagnet, but the Hamiltonian preserves the full point-group symmetry of the square lattice:

$$H_s = \sum_{j<k} J_{jk} \left(\hat{\sigma}_j^x \hat{\sigma}_k^x + \hat{\sigma}_j^y \hat{\sigma}_k^y + \hat{\sigma}_j^z \hat{\sigma}_k^z \right) + \ldots \tag{17}$$

Here the $J_{jk} > 0$ are short-range exchange interactions which preserve the square lattice symmetry, and the ellipses represent possible further multiple spin terms. Now imagine tuning all the non-nearest-neighbor terms as a function of some generic coupling constant g. For small g, when H_s is nearly the square lattice antiferromagnet, the ground state has antiferromagnetic order as in Fig 4 and Eqn. (11). What is now the 'disordered' ground state for large g? One natural candidate is the spin-singlet paramagnet in Fig 2. However, because all nearest neighbor bonds of the square lattice are now

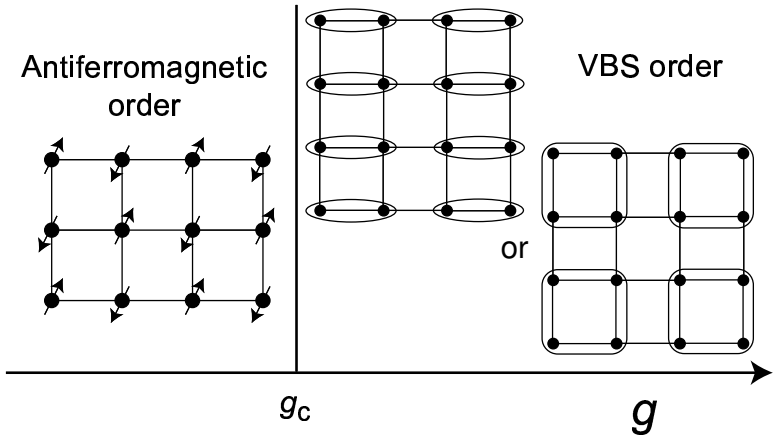

Figure 6: Phase diagram of H_s. Two possible VBS states are shown: one which is the analog Fig 2, and the other in which spins form singlets in a plaquette pattern. Both VBS states have a four-fold degeneracy due to breaking of square lattice symmetry. So the novel critical point at $g = g_c$ (described by $\mathcal{Z}_z$) has the antiferromagnetic and VBS orders vanishing as it is approached from either side: this co-incident vanishing of orders is generically forbidden in LGW theories.

equivalent, the state in Fig 2 is degenerate with 3 other states obtained by successive 90 degree rotations about a lattice site. In other words, the state in Fig 2, when transferred to the square lattice, *breaks* the symmetry of lattice rotations by 90 degrees. Consequently it has a new type of order, often called valence-bond-solid (VBS) order. It is now believed [i] that a large class of models like H_s do indeed exhibit a second-order quantum phase transition between the antiferromagnetic state and a VBS state—see Fig 6. Both the existence of VBS order in the paramagnet, and of a second-order quantum transition, are features that are not predicted by LGW theory: these can only be understood by a careful study of quantum interference effects associated with Berry phases of spin fluctuations about the antiferromagnetic state.

We will now review the manner in which Berry phases lead to a breakdown of LGW field theory. We begin with the field theory $\mathcal{Z}_\phi$ in Eq. (12) for the coupled dimer antiferromagnet, and modify it to include Berry phases of the spin. For each spin, the partition function acquires a phase factor $e^{iA/2}$, where A is the area enclosed by the world-line of the spin on the unit sphere in spin space. To include this contribution, it is necessary to rewrite Eq. (12) in terms of a "hard-spin" unit vector field $\mathbf{n}$, rather than the

soft-spin field ϕ_α. The direction of $\mathbf{n}$ then represents the local orientation of the antiferromagnetic order parameter. Furthermore, the Berry phase contributions oscillate rapidly from site to site, and so we have to write them down on the underlying lattice, and cannot directly take the continuum limit. In this manner, we obtain from Eq. (12)

$$\begin{aligned} \mathcal{Z}_{\mathbf{n}} &= \int \mathcal{D}\mathbf{n}(r,\tau)\delta(\mathbf{n}^2(r,\tau)-1)\exp\Bigg[\frac{i}{2}\sum_j \eta_j \int d\tau \mathcal{A}_\tau(\mathbf{n}(r_j,\tau)) \\ &\qquad - \frac{1}{2gc}\int d^2r d\tau \left((\partial_\tau \mathbf{n})^2 + c^2(\nabla_r \mathbf{n})^2\right)\Bigg], \end{aligned} \tag{18}$$

Excluding the first Berry phase term, this is the action of the so-called O(3) non-linear sigma model in 3 spacetime dimensions. Here we are primarily interested in the consequences of the Berry phases: $\mathcal{A}_\tau(\mathbf{n}(\tau))d\tau$ is defined to be the oriented area of the spherical triangle defined by $\mathbf{n}(\tau)$, $\mathbf{n}(\tau + d\tau)$, and an arbitrary reference point $\mathbf{n}_0$ (which is usually chosen to be the north pole).

The theory (18) can be considered to be the "minimal model" of quantum antiferromagnets on the square lattice. At small g there is the conventional magnetically ordered "Néel" phase with $\langle \mathbf{n} \rangle \neq 0$, while at large g there is a "quantum disordered" paramagnetic phase which preserves spin rotation invariance with $\langle \mathbf{n} \rangle = 0$. We are especially interested here in the nature of this paramagnetic state.

The key to an analysis of the large g regime is a better understanding of the nature of $\mathcal{A}_\tau$. We will see that $\mathcal{A}_\tau$ behaves in many respects like the time-component of a compact U(1) gauge field, and indeed, this accounts for the suggestive notation. All physical results should be independent of the choice of the reference point $\mathbf{n}_0$, and it is easy to see by drawing triangles on the surface of a sphere that changes in $\mathbf{n}_0$ amount to gauge transformations of $\mathcal{A}_\tau$. If we change $\mathbf{n}_0$ to $\mathbf{n}_0'$, then the resulting $\mathcal{A}_\tau'$ is related to $\mathcal{A}_\tau$ by

$$\mathcal{A}_\tau' = \mathcal{A}_\tau - \partial_\tau \phi(\tau) \tag{19}$$

where $\phi(\tau)$ measures the oriented area of the spherical triangle defined by $\mathbf{n}(\tau)$, $\mathbf{n}_0$, and $\mathbf{n}_0'$. Furthermore, as we will discuss more completely below, the area of any spherical triangle is uncertain modulo 4π, and this accounts for the 'compactness' of the U(1) gauge theory.

We proceed with our analysis of $\mathcal{Z}_{\mathbf{n}}$. First, we discretize the gradient terms of the O(3) sigma model. We will limit our considerations here to antiferromagnets on the square lattice, but similar considerations apply to other bipartite lattices. We also discretize the imaginary time direction, and (by a slight abuse of notation) use the same index j to refer to the sites of a 3 dimensional cubic lattice in spacetime. On such a lattice we can rewrite (18) as

$$\mathcal{Z}_{\mathbf{n}} = \int \prod_j d\mathbf{n}_j \delta(\mathbf{n}_j^2 - 1) \exp\left(\frac{1}{2g} \sum_{j,\mu} \mathbf{n}_j \cdot \mathbf{n}_{j+\hat{\mu}} + \frac{i}{2} \sum_j \eta_j \mathcal{A}_{j\tau} \right), \qquad (20)$$

where the sum over μ extends over the 3 spacetime directions, and $\mathcal{A}_{j\mu}$ is defined to equal the oriented area of the spherical triangled formed by $\mathbf{n}_j$, $\mathbf{n}_{j+\mu}$ and the arbitrary (but fixed) reference point $\mathbf{n}_0$. We have also dropped unimportant factors of the lattice spacing and the spin-wave velocity in (20).

The theory Eq. (20) is still cumbersome to work with because $\mathcal{A}_{j\tau}$ is a complicated function of the $\mathbf{n}_j$. However, a purely local formulation can be found by re-expressing $\mathbf{n}_j$ in terms of *spinor* variables. We write

$$n_{j\alpha} = z_{ja}^* \sigma_{ab}^{\alpha} z_{jb}, \qquad (21)$$

where σ^{α} are the Pauli matrices, the z_{ja} are two-component complex spinor fields residing on the sites of the cubic lattice, and a is a *spinor* index which extends over $\uparrow, \downarrow$. It is an interesting classical result in spherical trigonometry that the area of a spherical triangle can be expressed quite simply in terms of the spinor co-ordinates of its vertices. We will not explicitly review this analysis here, but refer the reader to a separate review [j]. Using this result, it is not difficult to show that Eq. (20) is very closely related to the following partition function on the cubic lattice

$$\begin{aligned} \mathcal{Z}_z &= \prod_{j\mu} \int_0^{2\pi} \frac{dA_{j\mu}}{2\pi} \prod_{ja} \int dz_{ja} \prod_j \delta\left(|z_{ja}|^2 - 1 \right) \\ &\qquad \exp\left(\frac{1}{g} \sum_{j\mu} \left(z_{ja}^* e^{-iA_{j\mu}} z_{j+\mu,a} + \text{c.c.} \right) + i \sum_j \eta_j A_{j\tau} \right). \qquad (22) \end{aligned}$$

Note that we have introduced a new field $A_{j\mu}$, on each link of the cubic lattice, which is integrated over. This is a compact U(1) gauge field which

has replaced $\mathcal{A}_{j\mu}$ in Eq. (20): it can be shown [j] that the integral over $A_{j\mu}$ in Eq. (22) is dominated by values $A_{j\mu} \approx \mathcal{A}_{j\mu}/2$, and the resulting action differs from Eq. (20) only in unimportant details. The crucial advantage of Eq. (22) is, of course, that there are no constraints between the z_{ja} and the $A_{j\mu}$, and we now we have to deal with a purely local lattice gauge theory.

The theory $\mathcal{Z}_z$ now allows us to address the key questions linked to the breakdown of LGW theory. At small g, we have, as before, a Néel state with $\langle z_a \rangle \neq 0$, and hence from Eq. (21) $\langle \mathbf{n} \rangle \neq 0$. We will now describe the nature of the large g paramagnetic phase, and of the transition between the small and large g phases in the subsections below.

4.1 Nature of the paramagnet

For large g, there are strong fluctuations of the z_{ja}, and it therefore pays to integrate out the z_{ja} from $\mathcal{Z}_z$ and obtain an effective theory for the $A_{j\mu}$. This can be done order-by-order in $1/g$ in a "high temperature" expansion. The powers of $1/g$ yield terms dependent upon gauge-invariant U(1) fluxes on loops of all sizes residing on the links of the cubic lattice. For our purposes, it is sufficient to retain only the simplest such term on elementary square plaquettes, yielding the partition function

$$\mathcal{Z}_A = \prod_{j\mu} \int_0^{2\pi} \frac{dA_{j\mu}}{2\pi} \exp\left(\frac{1}{e^2} \sum_{\square} \cos\left(\epsilon_{\mu\nu\lambda} \Delta_\nu A_{j\lambda}\right) + i \sum_j \eta_j A_{j\tau} \right), \qquad (23)$$

where $\epsilon_{\mu\nu\lambda}$ is the totally antisymmetric tensor in three spacetime dimensions. Here the cosine term represents the conventional Maxwell action for a compact U(1) gauge theory: it is the simplest local term consistent with the gauge symmetry and which is periodic under $A_{j\mu} \to A_{j\mu} + 2\pi$. The sum over $\square$ in (23) extends over all plaquettes of the cubic lattice, Δ_μ is the standard discrete lattice derivative ($\Delta_\mu f_j \equiv f_{j+\mu} - f_j$ for any f_j), and e^2 is a coupling constant. We expect the value of e to increase monotonically with g.

The properties of a pure compact U(1) theory have been described by Polyakov [k]. Here we need to extend his analysis to include the all-important Berry phases in $\mathcal{Z}_A$. The Berry phase has the interpretation of a $\int J_\mu A_\mu$ coupling to a static matter field with 'current' $J_\mu = \delta_{\mu\tau}$ *i.e.* static charges ± 1 on the two sublattices. It is this matter field which will crucially control the nature of the paramagnet.

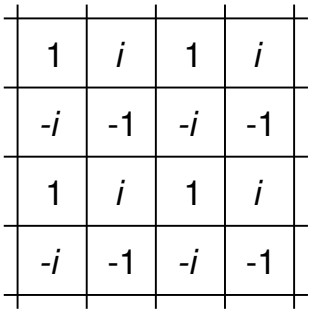

Figure 7: The values of the fixed field ζ_i, which specify the Berry phase of the monopole tunnelling events. The monopoles are assumed to be centered on the sites of the dual lattice.

Polyakov showed that the quantum fluctuations of the pure compact U(1) gauge theory were controlled by *monopole* tunnelling events at which the U(1) gauge flux changed by 2π. In particular, at all values of the coupling e, the monopoles eventually proliferate at long enough distances and lead to confinement of 'electric' charges: here these electric charges are the $S = 1/2$ z_a quanta (also known as 'spinons').

For our purposes, we need to understand the influence of the Berry phase terms in $\mathcal{Z}_A$ on the monopoles. This is a subtle computation [l, m] which has been reviewed elsewhere [j]. The final result is that each monopole can also be associated with a Berry phase factor. If $m_j^\dagger$ is the monopole creation at site j, then this appears in the partition function as

$$m_j^\dagger \zeta_j \tag{24}$$

where ζ_j is a fixed field taking the values 1, i, -1, $-i$ on the four square sublattices as shown in Fig 7.

An important consequence of these Berry phases is that the monopole operator now transforms non-trivially under the operations of the square lattice space group. Indeed, the partition function of the antiferromagnet must be invariant under all space group operations, and so by demanding the invariance of Eq. (24), we deduce the transformation properties of the monopole operator. A simple analysis of Eq. (24) then shows that

$$\begin{aligned} T_x &: m \to i m^\dagger \\ T_y &: m \to -i m^\dagger \end{aligned}$$

$$\begin{aligned} R^{\rm dual}_{\pi/2} &: m \to m^\dagger \\ I^{\rm dual}_x &: m \to m \\ \mathcal{T} &: m \to m. \end{aligned} \tag{25}$$

Here $T_{x,y}$ are translations by one lattice spacing along the $x.y$ axes, $R^{\rm dual}_{\pi/2}$ is a rotation by $\pi/2$ about a site of the dual lattice, $I^{\rm dual}_x$ is reflection about the y axis of the dual lattice, and $\mathcal{T}$ is time-reversal.

The transformation properties in Eq. (25) now allow us to relate the monopole operator to physical observables by searching for combinations of spin operators which have the same signature under space group operations. It turns out that the monopole operator is connected to the VBS order parameter [m]. From Fig 6, we note that VBS order is associated with modulations in the value of the nearest-neighbor spin-singlet correlations. So we can define a complex order parameter, $\psi_{\rm VBS}$, such that

$$\begin{aligned} {\rm Re}\left[\psi_{\rm VBS}\right] &= (-1)^{j_x} \sum_\alpha \hat\sigma^\alpha_j \hat\sigma^\alpha_{j+x} \\ {\rm Im}\left[\psi_{\rm VBS}\right] &= (-1)^{j_y} \sum_\alpha \hat\sigma^\alpha_j \hat\sigma^\alpha_{j+y}. \end{aligned} \tag{26}$$

It is now easy to work out the space group transformations of $\psi_{\rm VBS}$. These lead to the important correspondence [m, i]

$$m \sim e^{-i\pi/4} \psi_{\rm VBS}. \tag{27}$$

We have now assembled all the ingredients necessary to describe the interplay between the monopole dynamics and Berry phases in the paramagnetic phase. Using a mapping from the compact U(1) gauge theory to a dual effective action for monopoles, the proliferation of monopoles can be argued [j] to be equivalent to their "condensation" with $\langle m_j \rangle \neq 0$. This argument also applies in the presence of Berry phases, although cancellations among the phases now leads to a significantly smaller value of $\langle m_j \rangle$. Nevertheless, it can be shown that $\langle m_j \rangle$ is non-zero in the paramagnetic phase. Because of the non-trivial transformation properties of m_j under the square lattice space group noted above, it is then clear that a non-zero $\langle m_j \rangle$ spontaneously breaks the space group symmetry. Indeed, the connection in Eq. (27) shows that this broken symmetry is reflected in the appearance of VBS order. The precise configuration of the VBS order depends upon the value of Arg$[\langle m \rangle]$.

Using Eq. (27) and the space group transformations above, the two VBS configurations shown in Fig. 6 appear for $\mathrm{Arg}[\langle m \rangle]$ equal to $\pi/4, 3\pi/4, 5\pi/4, 7\pi/4$ or $0, \pi/2, \pi, 3\pi/2$.

We have now established the breakdown of LGW theory induced by the Berry phases in $\mathcal{Z}_{\mathbf{n}}$ in Eq. (18). A theory of the quantum fluctuations of the LGW antiferromagnetic order parameter $\mathbf{n}$ does not lead to featureless 'quantum disordered' paramagnetic state. Rather, subtle quantum interference effects induce a new VBS order parameter and an associated broken symmetry.

4.2 Deconfined criticality

We now turn to a brief discussion of the quantum phase transition between the small g Néel phase with $\langle \mathbf{n} \rangle \neq 0$ and $\langle \psi_{\mathrm{VBS}} \rangle = 0$ and the large g paramagnetic phase with $\langle \mathbf{n} \rangle = 0$ and $\langle \psi_{\mathrm{VBS}} \rangle \neq 0$. The two phases are characterized with two apparently independent order parameters, transforming very differently under spin and lattice symmetries. Given these order parameters, LGW theory predicts that there can be no direct second-order phase transition between them, except with fine tuning.

Recent work by Senthil *et al.* [i] has shown that this expectation is incorrect. Central to their argument is the demonstration that at a possible quantum critical point, the monopole Berry phases in Eq. (24) lead to complete cancellation of monopole effects even at the longest distance scales. Recall that in the $g > g_c$ paramagnetic phase, Berry phases did lead to a partial cancellation of monopole contributions, but a residual effect was present at the longest scales. In contrast, the monopole suppression is complete at the $g = g_c$ quantum critical point.

With the suppression of monopoles, the identification of the continuum critical theory turns out to be quite straightforward. We simply treat $A_{j\mu}$ as a non-compact U(1) gauge field, and take the naive continuum limit of the action $\mathcal{Z}_z$ in Eq. (22) while ignoring both monopoles and their Berry phases. This leads to the field theory

$$\mathcal{Z}_{zc} = \int \mathcal{D}z_a(x,\tau)\mathcal{D}A_\mu(x,\tau) \exp\Bigg(- \int d^2x d\tau \Big[|(\partial_\mu - iA_\mu) z_a|^2 + s|z_a|^2 + \frac{u}{2}(|z_a|^2)^2 + \frac{1}{2e^2}(\epsilon_{\mu\nu\lambda}\partial_\nu A_\lambda)^2 \Big] \Bigg). \tag{28}$$

In comparing $\mathcal{Z}_{zc}$ to the continuum theory $\mathcal{Z}_\phi$ for the coupling dimer antiferromagnet, note that the vector order parameter ϕ_α has been replaced by a spinor z_a, and these are related by $\phi_\alpha \sim z_a^* \sigma^\alpha_{ab} z_b$, from Eq. (21). So the order parameter has *fractionalized* into the z_a spinons. A second novel property of $\mathcal{Z}_z$ is the presence of a U(1) gauge field A_μ: this gauge field emerges near the critical point, even though the underlying model in Eqn (17) only has simple two spin interactions.

Studies of fractionalized critical theories like $\mathcal{Z}_{zc}$ in other models with spin and/or charge excitations is an exciting avenue for further theoretical research, and promises to have significant applications to a variety of correlated electron systems [n, o].

References

[a] S. Sachdev, *Quantum Phase Transitions* in *Encyclopedia of Mathematical Physics*, edited by J.-P. Francoise, G. Naber, and T. S. Tsun, Elsevier, Amsterdam (2005).

[b] D. Bitko, T. F. Rosenbaum, and G. Aeppli, *Quantum Critical Behavior for a Model Magnet*, Phys. Rev. Lett. **77**, 940 (1996).

[c] H. Tanaka, A. Oosawa, T. Kato, H. Uekusa, Y. Ohashi, K. Kakurai, and A. Hoser, *Observation of Field-Induced Transverse Nel Ordering in the Spin Gap System $TlCuCl_3$*, J. Phys. Soc. Jpn. **70**, 939 (2001).

[d] A. Oosawa, M. Fujisawa, T. Osakabe, K. Kakurai, and H. Tanaka, *Neutron Diffraction Study of the Pressure-Induced Magnetic Ordering in the Spin Gap System $TlCuCl_3$*, J. Phys. Soc. Jpn **72**, 1026 (2003).

[e] Ch. Rüegg, N. Cavadini, A. Furrer, H.-U. Güdel, K. Krämer, H. Mutka, A. Wildes, K. Habicht, and P. Vorderwisch, *Bose-Einstein condensation of the triplet states in the magnetic insulator $TlCuCl_3$*, Nature (London) **423**, 62 (2003).

[f] M. Matsumoto, B. Normand, T. M. Rice, and M. Sigrist, *Magnon Dispersion in the Field-Induced Magnetically Ordered Phase of* $TlCuCl_3$,

Phys. Rev. Lett. **89**, 077203 (2002) and *Field- and pressure-induced magnetic quantum phase transitions in $TlCuCl_3$*, Phys. Rev. B **69**, 054423 (2004).

[g] M. Matsumoto, C. Yasuda, S. Todo, and H. Takayama, *Ground-state phase diagram of quantum Heisenberg antiferromagnets on the anisotropic dimerized square lattice*, Phys. Rev. B **65**, 014407 (2002).

[h] S. Sachdev, *Quantum Phase Transitions*, Cambridge University Press, Cambridge (1999).

[i] T. Senthil, A. Vishwanath, L. Balents, S. Sachdev, and M. P. A. Fisher, *Deconfined Quantum Critical Points*, Science **303**, 1490 (2004); T. Senthil, L. Balents, S. Sachdev, A. Vishwanath, and M. P. A. Fisher, *Quantum criticality beyond the Landau-Ginzburg-Wilson paradigm*, Phys. Rev. B **70**, 144407 (2004).

[j] S. Sachdev in *Quantum magnetism*, U. Schöllwock, J. Richter, D. J. J. Farnell and R. A. Bishop eds, Lecture Notes in Physics, Springer, Berlin (2004), cond-mat/0401041.

[k] A. M. Polyakov, *Gauge Fields and Strings*, Harwood Academic, New York (1987).

[l] F. D. M. Haldane, *O(3) Nonlinear σ Model and the Topological Distinction between Integer- and Half-Integer-Spin Antiferromagnets in Two Dimensions*, Phys. Rev. Lett. **61**, 1029 (1988).

[m] N. Read and S. Sachdev, *Spin-Peierls, valence-bond solid, and Nel ground states of low-dimensional quantum antiferromagnets*, Phys. Rev. B **42**, 4568 (1990).

[n] T. Senthil, S. Sachdev, and M. Vojta, *Quantum phase transitions out of the heavy Fermi liquid*, Physica B **359-361**, 9 (2005).

[o] L. Balents, L. Bartosch, A. Burkov, S. Sachdev, and K. Sengupta, *Putting competing orders in their place near the Mott transition*, Phys. Rev. B **71**, 144508 (2005).